CRYSTAL GROWTH & DESIGN

Article

pubs.acs.org/crystal

Ligand-Driven Anion−π Interaction-Induced Silver(I) Coordination Chemistry

Damir A. Safin,*[,†] Koen Robeyns,[†] Maria G. Babashkina,[†] Christophe M. L. Vande Velde,[‡] and Yaroslav Filinchuk[†]

[†]Institute of Condensed Matter and Nanosciences, Molecules, Solids and Reactivity (IMCN/MOST), Université catholique de Louvain, Place L. Pasteur 1, 1348 Louvain-la-Neuve, Belgium

[‡]Faculty of Applied Engineering, Advanced Reactor Technology, University of Antwerp, Groenenborgerlaan 171, 2020 Antwerp, Belgium

Supporting Information

ABSTRACT: Three novel coordination compounds were successfully isolated using rare and poorly studied 5-phenyl-2,2′-bipyridine (L^I) and completely unexplored 6-phenyl-3-(pyridin-2-yl)-1,2,4-triazine (L^{II}) ligands with $AgNO_3$, namely, $[Ag(L^I)_2]NO_3·0.5H_2O$ (**1**), $[Ag(L^I)PPh_3NO_3]·0.5CH_2Cl_2$ (**2**), and $[Ag_2(L^{II})_2(H_2O)_2](NO_3)_2$ (**3**). **1** can be converted into **2** upon reacting with PPh_3, while no conversion was observed for **3**. The formation of **3** was templated through anion−π-system interactions between the NO_3^- anions and the electron deficient 1,2,4-triazine ring of L^{II}, which play a crucial role in the supramolecular assembly.

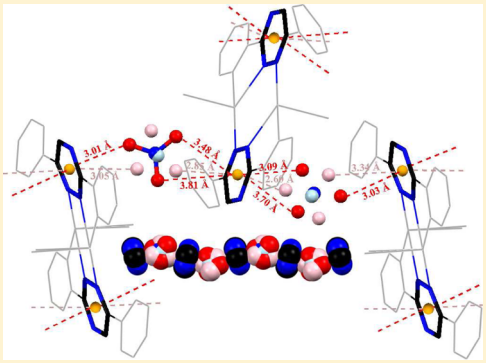

INTRODUCTION

Almost 20 years ago, pioneering theoretical investigations revealed that it is possible to have efficient interactions between a π-acidic aromatic ring and an electron-rich molecule.[1,2] Since these breakthrough studies a new type of noncovalent contacts associated with aromatic rings, namely, anion−π interaction, has received significant interest due to its fundamental role in biological and chemical applications.[3−16] Thereafter, it was established that anion−π interactions are energetically favorable (~20−70 kJ/mol).[17−19] Recently, the first crystallographic evidence of anion interaction with aromatic receptors has been described.[20,21] Since these pioneering experimental results, a great number of structures with anion−π interactions have been obtained, although these contacts often had largely been overlooked by the original authors. Furthermore, the physical nature of the anion−π interaction has also been extensively analyzed.[17−19,22−25] From these studies, it has been concluded that electrostatic forces and ion-induced polarization are the main energetic contributors to the anion−π complex. However, it has also been demonstrated that the ability of a phenyl ring with electron-withdrawing substituents to bind an anion is not a result of changes in interaction of the anion with the phenyl ring itself. Instead, it is due to favorable interactions of the anion with the substituents that overwhelm the unfavorable interactions of the anion with the ring.[26,27] A similar model can describe different anion-binding abilities of *N*-heterocycles.

Besides π-electron-deficient aromatic rings, comprising a benzene ring with strong electron withdrawing substituents, π-deficient six-membered heteroaromatics, being synthetically more versatile, are of ever-increasing interest.[5] The properties of the anion are also an important issue for anion−π bonding.[17−19] Small anions are more polarizing and present short ion-arene distances yielding more negative interaction energies. Planar and linear anions (e.g., NO_3^- or N_3^-) can interact with the aromatic ring through π−π stacking.

The influence of metal coordination to heteroaromatic rings on the efficiency of the anion−π interactions has been studied for pyridine, pyrazine, and *s*-tetrazine with Ag^I. Interestingly, based on high-level ab initio calculations, it was established that the anion binding properties of these heterocycles are dramatically enhanced when they are coordinated to Ag^I,[28] as well as the progressive enhancement of the π-acidity by increasing the number of Ag^I ions *N*-coordinated to tetrazine.[29] Further structural motifs of self-assembled Ag^I complexes, dictated by anion−π interactions, have also been reported for 3,6-bis(2-pyridyl)-1,2,4,5-tetrazine (bptz) and 3,6-bis(2-pyridyl)-1,2-pyridazine (bppn) with a number of closely related Ag^IX salts (X = PF_6^-, AsF_6^-, SbF_6^-, and BF_4^-).[30,31] A clear propensity to form propeller-type products $[Ag_2(bptz)_3]^{2+}$, exhibiting short anion−π contacts, versus preferentially favored grid-like structures $[Ag_4(bppn)_4]^{4+}$, which exhibit maximized π−π interactions, was established for bptz and less π-acidic

Received: February 19, 2016
Revised: May 11, 2016
Published: May 17, 2016

DOI: 10.1021/acs.cgd.6b00277
Cryst. Growth Des. 2016, 16, 3763−3770

Scheme 1. Syntheses of 1−3

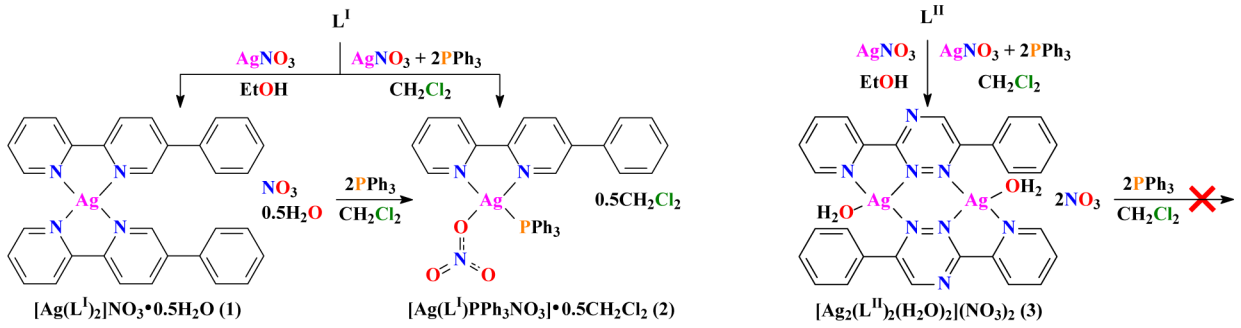

bppn, respectively. Using the anion−π interaction strategy, we have also reported the self-assembly of 3,6-bis(2′-pyrimidyl)-1,2,4,5-tetrazine (BPymTz) and 2,4,6-tris(2-pyrimidyl)-1,3,5-triazine (TPymT), whose renaissance was announced recently,[32−39] with $Ag^{I}X$ salts (X = PF_6^-, OTf^-, and ClO_4^-).[37] In all of the obtained complexes, the anion−π interactions between the anions and the electron deficient aromatic ligands play a crucial role in the self-assembly of the supramolecules. Thus, combination of ligands with π-electron-deficient aromatic rings and $Ag^{I}X$ salts is an efficient strategy to generate anion−π interactions. This is not only due to interactions between a π-acidic aromatic ring and an electron-rich anion, but also due the coordinative flexibility of the Ag^{I} ion.

With all this in mind and armed with knowledge on anion−π interactions, we have directed our attention to the interaction of $AgNO_3$ with 5-phenyl-2,2′-bipyridine ($\mathbf{L^I}$). This ligand is efficiently synthesized from its precursor, namely, 6-phenyl-3-(pyridin-2-yl)-1,2,4-triazine ($\mathbf{L^{II}}$),[40,41] which, in turn, is also a very attractive ligand for coordination chemistry. Before our investigations of $\mathbf{L^I}$,[42] only four crystal structures of its metal complexes have been known.[41,43−46] Even more telling is that nothing was reported about the complexation properties of $\mathbf{L^{II}}$ so far. This is surprising since the presence of the central 1,2,4-triazine ring in its structure can lead, in our opinion, to a rich variety of complexes with interesting properties as well as an efficient π-electron-deficient receptor for anions.[5]

In this contribution, we describe the synthesis and complete structural investigation of Ag^{I} complexes of $\mathbf{L^I}$ and $\mathbf{L^{II}}$, namely, $[Ag(L^I)_2]NO_3{\cdot}0.5H_2O$ (**1**), $[Ag(L^I)PPh_3NO_3]{\cdot}0.5CH_2Cl_2$ (**2**), and $[Ag_2(L^{II})_2(H_2O)_2](NO_3)_2$ (**3**), which were obtained through the direct reaction of the corresponding ligand with $AgNO_3$ (**1** and **3**) or with a mixture of $AgNO_3$ and PPh_3 (**2** and **3**) (Scheme 1). Furthermore, conversion of **1** to **2** upon reaction with PPh_3, while there is no conversion of **3** upon reaction with PPh_3, is also described (Scheme 1).

RESULTS AND DISCUSSION

Compound **1** crystallizes in the orthorhombic space group $P2_12_12$ due the apparent helicity around the metal center, caused by the geometric organization of the ligands. The crystals were, however, found to be twinned by inversion with a refined ratio of 40/60. As such both helical arrangements, with inverted chirality, coexist in the crystal. Complexes **2** and **3** both crystallize in the triclinic space group $P\bar{1}$. The bulk samples of **1**−**3** were studied by means of powder X-ray diffraction (Figure 1). The experimental X-ray powder patterns are in agreement with the calculated powder patterns obtained from the single crystal X-ray structures.

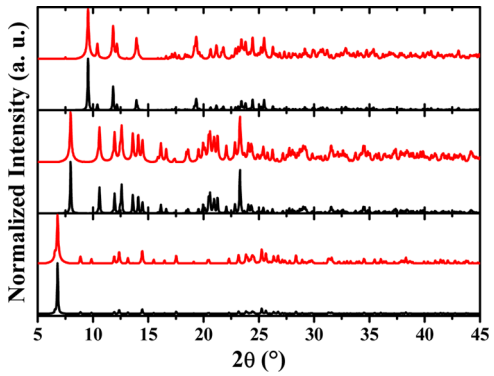

Figure 1. Normalized calculated (black) and experimental (red) X-ray powder diffraction patterns of **1** (bottom), **2** (middle), and **3** (top).

The structure of **1** consists of the discrete $[Ag(L^I)_2]^+{\cdot}0.5H_2O$ cation (Figure 2) and the noncoordinate NO_3^- anion, which is

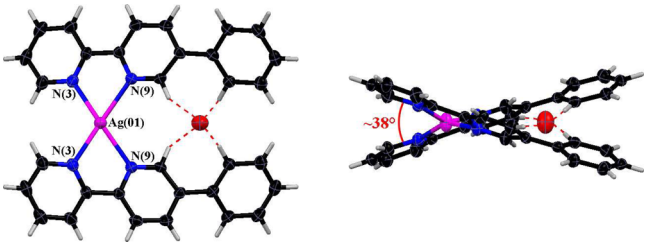

Figure 2. Top (left) and side (right) views on the $[Ag(L^I)_2]^+{\cdot}0.5H_2O$ cation in the structure of **1**. Color code: C = black, H = light gray, Ag = magenta, N = blue, O = red.

found in the void channels that penetrate the crystal structure along the *a*-axis. The anion was found to be disordered and refined as a rigid group over two sites. Given the absence of interactions with the $[Ag(L^I)_2]^+$ cation and the available space in the cavity it resides in, it is very possible that the NO_3^- anion can move freely throughout the whole void, although the electron density in the crystal suggests that it is principally found around the currently refined positions, where it competes with solvent molecules. The large anion thermal ellipsoids indicate imperfect modeling. The remaining electron density was treated with the squeeze algorithm in Platon,[47] which located about 36 electrons in each void column per unit cell, which could not be attributed to any discrete molecules, neither solvent nor partially occupied NO_3^- anions. The Ag^{I} cation is coordinated to two ligands via the 2,2′-bipyridine coordination pocket of $\mathbf{L^I}$ affording a tetracoordinate environment. The coordination polyhedron adopted by this environment is

DOI: 10.1021/acs.cgd.6b00277
Cryst. Growth Des. 2016, 16, 3763−3770

characterized using the τ_4-descriptor for four coordinated ions.[48] The distortion index is defined as $\tau_4 = (360 - \alpha - \beta)/141$, where α and β are the two largest bond angles around the metal ion. The τ_4 values for perfect tetrahedral, trigonal pyramid, seesaw structures and perfect square planar are 1.00, 0.85, 0.64−0.07, and 0.00, respectively. The τ_4 value of **1** is 0.4421 and indicates that the coordination geometry around Ag^I is best described as the seesaw structure. The Ag−N bond distances are within the range of 2.30−2.35 Å and the endocyclic N−Ag−N angles are 71.71(16)°, while the exocyclic N−Ag−N angles are 111.27(15)° and 116.75(17)°, and 154.94(18)° formed by the mono- and polytypic nitrogen atoms (Table S1 in the Supporting Information). The torsion angle between the least-squares planes formed by the 2,2′-bipyridine fragment, which, in turn, is essentially planar, and the phenyl ring of the same ligand is about 30°, while the same angles between two 2,2′-bipyridine fragments coordinate to the same metal center is about 38° (Figure 2).

Interestingly, every second $[Ag(L^I)_2]^+$ cation traps one water molecule, through hydrogen bonds of the C−H···OH_2 type (Table S2 in the Supporting Information), in the cavity formed by the coordination part and pendant phenyl fragments of the same molecule (Figure 2). Hydrogens on this water molecule could not be calculated or located in the difference Fourier map. All $[Ag(L^I)_2]^+$ cations in the structure of **1** are stacked parallel on top of each other, due to efficient $\pi-\pi$ stacking interactions (Table S3 in the Supporting Information) between the monotypic fragments of the ligands of adjacent $[Ag(L^I)_2]^+$ cations, with a weak $Ag^I\cdots Ag^I$ interaction of about 3.77 Å. As a result of these $\pi-\pi$ stacking interactions 1D pillars are formed along the *a* axis. These pillars are packed side-by-side along the *b* axis leading to 2D sheets. Two 2D sheets are further tail-to-tail packed and the resulting domains are separated from each other by 1D pillars of the disordered NO_3^- anions through the formation of hydrogen bonds of the C−H···ONO_2 type (Table S2 in the Supporting Information).

The asymmetric unit of **2** consists of the discrete $[Ag(L^I)PPh_3NO_3]$ molecule (Figure 3) and a half molecule of CH_2Cl_2, whose CH_2 group is disordered over two positions with an equal ratio. The Ag^I cation is coordinated to one ligand via the 2,2′-bipyridine coordination pocket of $\mathbf{L^I}$, one of the NO_3^- oxygen atoms and the PPh_3 phosphorus atom. The τ_4 value of **2** is 0.5525 and indicates that the coordination geometry around Ag^I is best described as the seesaw structure.

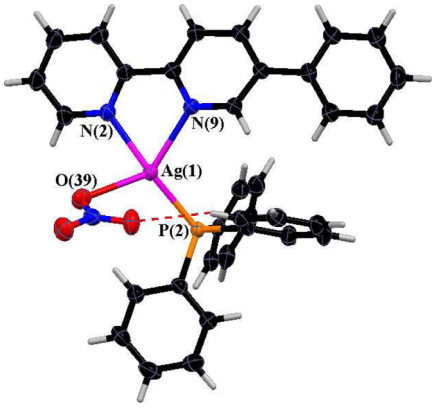

Figure 3. View on the $[Ag(L^I)PPh_3NO_3]$ molecule in the structure of **2**. Color code: C = black, H = light gray, Ag = magenta, N = blue, O = red, P = orange.

The Ag−N bond distances differ significantly and are of about 2.28 and 2.47 Å, while the Ag−O/P bond lengths are 2.52 and 2.36 Å, respectively (Table S4 in the Supporting Information). The N−Ag−N angle is 70.97(10)°, while the O/P−Ag−N angles are 80.15(11)° and 125.81(11)°, and 110.76(9)° and 156.29(9)°, respectively. Finally, the P−Ag−O angle is 113.64(7)°. Contrary to the structure of **1**, the 2,2′-bipyridine fragment of the ligand $\mathbf{L^I}$ in the structure of **2** significantly deviates from planarity with the torsion angle between the least-squares planes formed by two pyridine rings, being about 28°. At the same time the terminal pyridine and phenyl rings are essentially planar.

The crystal structure of **2** is stabilized by a linear intramolecular hydrogen bond of the C−H···ONO_2 type, which is formed between the hydrogen atom of one of the PPh_3 phenyl fragments and one of the noncoordinated oxygen atoms of the NO_3^- anion (Figure 3, Table S2 in the Supporting Information). Furthermore, linear intermolecular hydrogen bonds of the C−H···ONO_2 type are also found in the structure of **2** (Table S2 in the Supporting Information). Notably, two molecules of **2** are further linked through efficient $\pi-\pi$ stacking interactions (Table S3 in the Supporting Information), which are formed by each aromatic ring of the ligand $\mathbf{L^I}$, yielding a centrosymmetric dimer.

The structure of **3** comprises two independent discrete centrosymmetric dinuclear heteroleptic $[Ag_2(L^{II})_2(H_2O)_2]^{2+}$ cations (Figure 4) and two independent noncoordinate NO_3^- anions, which are disordered over two positions with 71% and 29%, and 83% and 17% ratios, respectively. Each $\mathbf{L^{II}}$ ligand is coordinated to one metal center via the 2,2′-bipyridine-like coordination pocket, formed by the nitrogen atom of the pyridine fragment and an adjacent nitrogen atom of the azine fragment of the 1,2,4-triazine ring, while the second azine nitrogen atom is linked to the second metal center. As a result of this coordination, $\mathbf{L^{II}}$ exhibits a bridging μ_2-coordination mode (Figure 4). Each Ag^I coordinates three nitrogen atoms, two of which arise from the 2,2′-bipyridine-like coordination pocket of one $\mathbf{L^I}$, while the third nitrogen corresponds to the triazine ring of the second $\mathbf{L^I}$ (Figure 2). The Ag−N(pyridine) and Ag−N(triazine) distances within the 2,2′-bipyridine-like coordination pocket are about 2.26 and 2.44 Å, respectively, while the remaining Ag−N(triazine) bond lengths are ∼2.24 Å (Table S5 in the Supporting Information). The coordination sphere of each Ag^I is completed to a tetracoordinate environment by the oxygen atom of the coordinated water molecules, which, in turn, are disordered in the structure of one of the independent molecules over two positions with a 65% and 35% ratio. The τ_4 values of two independent molecules of **3** are 0.5274 and 0.5391, respectively, and clearly indicate the seesaw structure. The N−Ag−N angles within the chelate fragments are about 71°, while the remaining N−Ag−N bond angles around the same metal center are ∼123° and ∼161° (Table S5 in the Supporting Information). The Ag−O bonds in the first molecule of **3** are almost orthogonal, while the same bonds in the second molecule are significantly tilted to the least-squares plane of the $[Ag_2(L^{II})_2]^{2+}$ species, which is reflected in the corresponding O−Ag−N bond angles (Table S5 in the Supporting Information) as well as O−Ag···Ag angles (Figure 4). The torsion angles between the planes formed by the pyridine and triazine, triazine and phenyl, and pyridine and phenyl rings in the structure of the first molecule of **3** are about 11°, 40°, and 51°, respectively. The same angles in the structure of the second molecule are 14°, 30°, and 16°, respectively.

DOI: 10.1021/acs.cgd.6b00277
Cryst. Growth Des. 2016, 16, 3763−3770

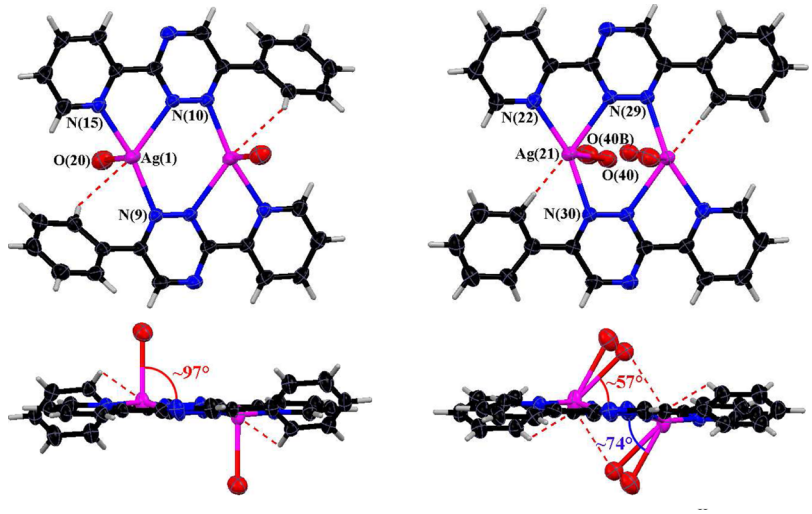

Figure 4. Top (top row) and side (bottom row) views on the $[Ag(L^{II})_2(H_2O)_2]^+$ cations in the structures of two independent molecules of **3**. Color code: C = black, H = light gray, Ag = magenta, N = blue, O = red.

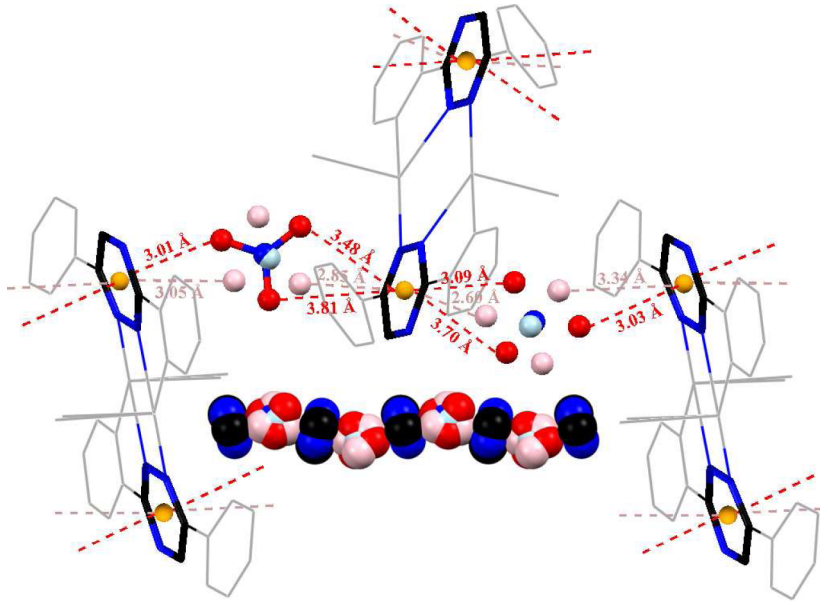

Figure 5. Ball and stick representations of a 1D chain, formed through anion−π contacts between NO_3^- anions and 1,2,4-triazine rings in the structure of **3**. Spacefill representation of a 1D pillar, constructed from stacked NO_3^- anions and 1,2,4-triazine rings. Disordered NO_3^- anions are shown with different color codes (N = blue, O = red for major occupancy, and N = light blue, O = pink for minor occupancy) to be clearly distinguished from each over.

Thus, the L^{II} ligands in the latter molecule are more planar than in the former one (Figure 4).

The observed coordination environments of the Ag^I atoms, observed within both independent molecules of **3**, can be reconsidered by close inspection of additional weak interactions of metal centers with one of the *ortho*-Ph hydrogen atoms (Figure 4) with the following parameters: d(Ag···H) = 2.64 and 2.66 Å, ∠(C−H···Ag) = 115° and 122° for the first and second independent molecules, respectively. Three forms of C−H···M interactions, namely, hydrogen bond, agostic, and anagostic, were reported.[49−57] Hydrogen bonds are 3-center-4-electron interactions with an almost linear geometry. Agostic interactions are 3-center-2-electron interactions and characterized by their short M···H distance (1.8−2.2 Å) and C−H···M bond angles (90−130°). Anagostic interactions are largely electrostatic in nature and characterized by long M···H distance (2.3−2.9 Å) and large C−H···M bond angles (110−170°). The observed C−H···Ag parameters in the structure of **3** nicely fit those for the anagostic interactions. Thus, the coordination numbers of each Ag^I can further be expanded due to relatively weak interactions with *ortho*-Ph hydrogen atoms. Due to these interactions, the metal cations now exhibit a pentacoordinated geometry (Figure 4). This coordination geometry can be described either as square-pyramidal or trigonal bipyramidal depending on the parameter $\tau_5 = (\alpha - \beta)/60$, where α and β are the two largest bond angles around the metal ion. An ideal square pyramidal arrangement is described by the value of τ = 0, while an ideal trigonal bipyramidal arrangement has the value of τ = 1.[58] The τ_5 value of the first molecule of **3** is 0.0132 and indicates that the coordination geometry around Ag^I is almost ideal square pyramidal. The same values for the second molecule, considering the disordered oxygen atoms, are 0.2753

DOI: 10.1021/acs.cgd.6b00277
Cryst. Growth Des. 2016, 16, 3763−3770

Table 1. NO_3^-–π Interaction Distances (Å) and Angles (deg) for 3[a]

interaction[b]	d(O···ring centroid)	d(O···ring plane)	∠(O···ring centroid axis and ring plane)	d(O···closest ring atom)
N(41)–O(42)···Cg(9)#1	3.810(18)	3.648	73.22	3.646 [C(13)]
N(41)–O(43)···Cg(9)#1	3.481(14)	3.329	72.99	3.357(14) [N(10)]
N(41)–O(44)···Cg(4)#2	3.005(12)	2.980	82.64	3.136(13) [N(33)]
N(41B)–O(42B)···Cg(4)#2	3.05(3)	2.730	63.34	2.79(3) [C(28)]
N(41B)–O(43B)···Cg(9)#1	2.85(3)	2.760	75.68	2.87(3) [C(13)]
N(51)–O(52)···Cg(9)#1	3.095(9)	2.962	73.18	3.017(10) [N(10)]
N(51)–O(53)···Cg(4)#1	3.031(9)	2.947	76.49	3.056(11) [N(30)]
				3.064(11) [C(31)]
N(51)–O(54)···Cg(9)#1	3.704(10)	3.524	72.03	3.553(12) [C(13)]
N(51B)–O(52B)···Cg(9)#1	2.60(3)	2.570	82.64	2.78(3) [C(8)]
N(51B)–O(54B)···Cg(4)#1	3.34(6)	3.110	68.31	3.14(6) [C(31)]

[a]Cg(4): N(29)–N(30)–C(31)–N(32)–C(33)–C(28). Cg(9): N(9)–N(10)–C(11)–N(12)–C(13)–C(8). [b]Symmetry transformations used to generate equivalent atoms: #1 *x*, *y*, *z*; #2 *x*, *y*, − 1 + *z*.

and 0.2468 and are best described as being about 28% and 25% along the pathway of distortion from the ideal square pyramidal toward trigonal bipyramidal structure. The coordination environments of Ag(1) can further be expanded up to a distorted octahedral coordination due to the interactions with the η^2 Cg[C(17)–C(18)] fragment ($d \approx 3.3$ Å) of the pyridine ring, corresponding to a different molecule. A similar expansion of the coordination environments of Ag(21) can be considered due to interactions with the water molecules coordinated to the second metal cation of the same molecule (d(Ag···O) ≈ 3.01(5) Å) with the O–Ag···Ag angle being about 57° (Figure 4). However, in the latter case the coordination octahedron is much more distorted.

A remarkable and unique feature of the crystal structure of **3** is the encapsulation of the NO_3^- anions between the triazine rings of adjacent crystallographically independent $[Ag_2(L^{II})_2(H_2O)_2]^{2+}$ cations (Figure 5) yielding 2D sheets, which, in turn, are linked through a number of intermolecular hydrogen bonds of the C–H···ONO_2 and C–H···OH_2 types (Table S2 in the Supporting Information), as well as π–π stacking interactions (Table S3 in the Supporting Information). The major occupancy of each NO_3^- anions is held in place by a total of three anion–π interactions, where one anion oxygen atom interacts with one of the triazine rings of one $[Ag_2(L^{II})_2(H_2O)_2]^{2+}$ cation, while remaining oxygen atoms interact with one of the triazine rings of the second $[Ag_2(L^{II})_2(H_2O)_2]^{2+}$ cation (Figure 5). The minor occupancy of each NO_3^- anions is held in place by a total of two anion–π interactions (Table 1), formed between two oxygen atoms of the anion and two triazine rings of neighboring two $[Ag_2(L^{II})_2(H_2O)_2]^{2+}$ cations (Figure 5). Due to this kind of aggregation, each NO_3^- anion is sandwiched between the two triazine rings, arising from different cationic species, while each triazine is sandwiched between the two NO_3^- anions. As a result, 1D $[-(1,2,4\text{-triazine})-(NO_3^-)-(1,2,4\text{-triazine})-(NO_3^-)-]_n$ chains are formed (Figure 5).

Since the higher π-acidity of triazines results in more attractive interactions with negatively polarized atoms, the multiple *N*-coordination to metal ions as Lewis acids may be a factor influencing the ability of the aromatic triazine system for anion–π binding. With respect to this, the NO_3^- anions exhibit very efficient anion–π interactions with 1,2,4-triazines in the structure of **3** with corresponding O···closest ring atom separations ranging from 3.65 to down to 3.02 Å and even down to significantly low values of 2.78–2.87 Å (Table 1). This leads to exceptionally short anion–π separations with O···ring plane distances ranging from 2.57 to 3.65 Å and O···ring centroid distance from one of the record values, as revealed by a comprehensive study of the Cambridge Structural Database (CSD),[5,59,60] ever observed for anion–π interactions of 2.60 to 3.81 Å (Table 1). Thus, the observed anion–π interactions may be evaluated from moderate to remarkably strong.

The spatial orientation of the nitrate groups is also influenced by hydrogen bonds involving the hydrogens of the coordinated water molecules and the oxygens of the nitrate ions. Although the hydrogens of these water molecules could not be calculated or located in the difference Fourier map, the presence of the hydrogen bonds is suggested by short contacts O(water)···ONO_2 = 2.60(3)–2.89(4) Å.

We have also thoroughly analyzed crystal structures, deposited in the CSD,[59,60] to identify potential NO_3^-–π interactions produced by (hetero)aromatic six-membered rings, namely, phenyl (R1), pyridine (R2), pyridazine (R3), pyrimidine (R4), pyrazine (R5), 1,2,3-triazine (R6), 1,2,4-triazine (R7), 1,3,5-triazine (R8), 1,2,3,4-tetrazine (R9), 1,2,3,5-tetrazine (R10), 1,2,4,5-tetrazine (R11), pentazine (R12), and hexazine (R13). Although results of the same search have already been reported on the pages of this journal,[5] more than seven years have passed since that time, and the total number of entries in the CSD have tripled.[59,60] For our comprehensive search, we have applied the same structural constraints as recently reported.[5] From the 12167 entries containing at least one (hetero)aromatic six-membered ring and the NO_3^- anion, 1786 (14.7%) structures exhibit 2265 short NO_3^-–π contacts. Among 1786 entries, 243 structures with 284 contacts are produced by R1, 1122 structures with 1559 contacts are produced by R2, 32 structures with 50 contacts are produced by R3, 127 structures with 186 contacts are produced by R4, 132 structures with 230 contacts are produced by R5, 39 structures with 80 contacts are produced by R7, 71 structures with 71 contacts are produced by R8 and 20 structures with 35 contacts are produced by R11. No hits were found for the other heteroaromatic six-membered rings (R6, R9, R10, R12, and R13) with NO_3^-. Scatter plots of the O···ring centroid axis and ring plane angle versus the shortest O···ring distance reveal that for R1, the NO_3^-–π interactions are mostly weak (Figure 6). R2 shows notably stronger contacts than the R1. In the cases of more electron-poor arenes, such as R3–R5, R7, R8, and R11, which contain two or more nitrogen atoms, the interactions are mainly strong (Figure 6).

The NO_3^- anions in the structure of **3** form anion–π interactions exclusively with a 1,2,4-triazine (R7) ring, and due

DOI: 10.1021/acs.cgd.6b00277
Cryst. Growth Des. 2016, 16, 3763–3770

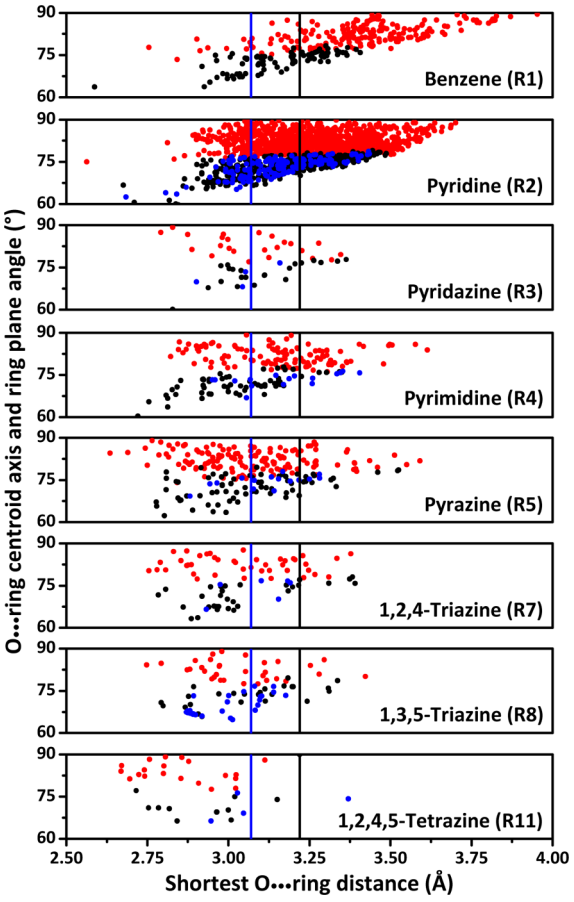

Figure 6. Scatter plot of the O···ring centroid axis and ring plane angle versus the shortest O···ring distance for NO_3^--aromatic pairs. The blue and the black lines represent the sum of the van der Waals radii N + O (3.07 Å) and C + O (3.22 Å),[61] respectively. The interactions between these two lines and to the left of the blue line are considered as significant and strong, respectively. Color code: red circle = the shortest contact is with the ring centroid, black circle = the shortest contact is with a carbon atom of the ring, blue circle = the shortest contact is with a nitrogen atom of the ring.

to the unique sandwich arrangement, several anion−π interactions can be identified. For each NO_3^- anion the shortest interaction is with the centroid of the 1,2,4-triazine ring. The corresponding range between 2.60 and 3.03 Å indicates a strong interaction, which is additionally stabilized by one other strong interaction for the N41B- and N51B-derived NO_3^- anions with a ring atom (less than the sum of the van der Waals radii N + O or C + O) or two weak interactions for the N41- and N51-derived NO_3^- anions (more than the sum of the van der Waals radii N + O or C + O). The shortest O···ring centroid distance in **3** (2.60 Å) is significantly shorter, while the above-mentioned weak interactions are significantly longer than what is found in the CSD (Figure 6).[59,60] The combination of two weaker interactions for the N41- and N51-derived NO_3^- anions might outbalance the strong second interaction observed for the N41B- and N51B-derived NO_3^- anions.

EXPERIMENTAL SECTION

Physical Measurements. Elemental analyses were performed on a PerkinElmer 2400 CHN analyzer.

Synthesis of $[Ag(L^I)_2]NO_3·0.5H_2O$ (1) and $[Ag_2(L^{II})_2(H_2O)_2](NO_3)_2$ (3, Path A). A solution of L^I or L^{II} (0.1 mmol; 23.2 and 23.4 mg, respectively) in EtOH (5 mL) was added dropwise under vigorous stirring to a solution of $AgNO_3$ (0.2 mmol, 34.0 mg) in EtOH (10 mL). The mixture was stirred at room temperature for 1 h and left for slow evaporation. X-ray suitable crystals were formed during the next day. Using other ratios of the corresponding ligand and $AgNO_3$ leads to the same complexes.

1. Colorless needle-like crystals. Yield: 29.3 mg (91%). Anal. Calcd for $C_{32}H_{25}AgN_5O_{3.5}$ (643.45) (%): C 59.73, H 3.92, and N 10.88; found: C 59.80, H 4.01, and N 10.82.

3. Colorless to pale yellow block-like crystals. Yield: 34.6 mg (82%). Anal. Calcd for $C_{28}H_{24}Ag_2N_{10}O_8$ (844.30) (%): C 39.83, H 2.87, and N 16.59; found: C 39.92, H 2.91, and N 16.65.

Synthesis of $[Ag_2(L^{II})_2(H_2O)_2](NO_3)_2$ (3, Path B). A solution of L^{II} (0.1 mmol; 23.4 mg) in CH_2Cl_2 (5 mL) was added dropwise under vigorous stirring to a mixture of $AgNO_3$ (0.2 mmol, 34.0 mg) and PPh_3 (0.4 mmol, 105.0 mg) in the same solvent (10 mL). The mixture was stirred at room temperature for 1 h. The solvent was then removed in vacuo. Complexes were isolated by recrystallization from a 1:4 mixture of CH_2Cl_2 and *n*-hexane. Using other ratios of L^{II}, $AgNO_3$ and PPh_3 lead to the same complex **3**.

3. Colorless to pale yellow block-like crystals. Yield: 32.1 mg (76%).

Synthesis of $[Ag(L^I)PPh_3NO_3]·0.5CH_2Cl_2$ (2). Path A. A solution of L^I (0.1 mmol, 23.2 mg) in CH_2Cl_2 (5 mL) was added dropwise under vigorous stirring to a mixture of $AgNO_3$ (0.2 mmol, 34.0 mg) and PPh_3 (0.4 mmol, 105.0 mg) in the same solvent (10 mL). The mixture was stirred at room temperature for 1 h. The solvent was then removed in vacuo. Complexes were isolated by recrystallization from a 1:4 mixture of CH_2Cl_2 and *n*-hexane. **Path B**. A solution of **1** (0.05 mmol, 32.6 mg) in CH_2Cl_2 (10 mL) was added dropwise under vigorous stirring to a solution of PPh_3 (0.1 mmol, 26.2 mg) in the same solvent (10 mL). The mixture was stirred at room temperature for 1 h. The solvent was then removed in vacuo. Complexes were isolated by recrystallization from a 1:4 mixture of CH_2Cl_2 and *n*-hexane.

2. Colorless rod-like crystals. Yield (Path A): 66.5 mg (94%). Anal. Calcd for $C_{34.5}H_{28}AgClN_3O_3P$ (706.92) (%): C 58.62, H 3.99, and N 5.94; found: C 58.49, H 4.11, and N 5.98. Yield (Path B): 30.8 mg (87%).

X-ray Powder Diffraction. X-ray powder diffraction for bulk samples was carried out using a MAR345 diffractometer equipped with a rotating anode (Mo$K\alpha$ radiation) and a XENOCS focusing mirror.

Single-Crystal X-ray Diffraction. X-ray data collection was performed on a Mar345 image plate detector using Mo $K\alpha$ radiation (Xenocs Fox3D mirror) at 150(2) K for **1** and **2**, and 297(2) K for **3**. The data were integrated with the CrysAlis(Pro) software.[62] The implemented empirical absorption correction was applied. The structures were solved by direct methods using the SHELXS or SHELXT program[63] and refined by full-matrix least-squares on $|F^2|$; using SHELXL-2014.[63] Non-hydrogen atoms were anisotropically refined and the hydrogen atoms were placed at calculated positions in riding mode with temperature factors fixed at 1.2 times U_{eq} of the parent atoms. Figures were generated using the program Mercury.[64]

Crystal Data for **1**. $C_{32}H_{24}AgN_4$, NO_3, $O_{0.5}$; M_r = 642.43 g mol^{-1}, orthorhombic, space group $P2_12_12$, a = 3.7687(3), b = 14.8455(8), c = 26.9112(17) Å, V = 1505.63(17) Å^3, Z = 2, ρ =

DOI: 10.1021/acs.cgd.6b00277
Cryst. Growth Des. 2016, 16, 3763−3770

1.417 g cm^{-3}, μ(Mo Kα) = 0.711 mm^{-1}, reflections: 9878 collected, 2824 unique, R_{int} = 0.040, R_1(all) = 0.0470, wR_2(all) = 0.1095.

Crystal Data for **2**. 2($C_{34}H_{27}AgN_3O_3P$), CH_2Cl_2; M_r = 1413.77 g mol^{-1}, triclinic, space group $P\bar{1}$, a = 9.6807(3), b = 12.9605(8), c = 14.4410(6) Å, α = 64.355(5), β = 82.252(3), γ = 69.979(5)°, V = 1534.48(15) Å^3, Z = 1, ρ = 1.530 g cm^{-3}, μ(Mo Kα) = 0.837 mm^{-1}, reflections: 19 452 collected, 5683 unique, R_{int} = 0.035, R_1(all) = 0.0458, wR_2(all) = 0.1041.

Crystal Data for **3**. $C_{28}H_{20}Ag_2N_8O_2$, 2(NO_3); M_r = 840.28 g mol^{-1}, triclinic, space group $P\bar{1}$, a = 8.8365(9), b = 11.925(3), c = 15.360(5) Å, α = 87.82(2), β = 77.108(16), γ = 80.770(14)°, V = 1557.3(7) Å^3, Z = 2, ρ = 1.792 g cm^{-3}, μ(Mo Kα) = 1.324 mm^{-1}, reflections: 11 817 collected, 5514 unique, R_{int} = 0.075, R_1(all) = 0.0837, wR_2(all) = 0.1836.

CONCLUSIONS

In summary, three novel coordination compounds were successfully isolated using 5-phenyl-2,2′-bipyridine ($\mathbf{L^I}$) and 6-phenyl-3-(pyridin-2-yl)-1,2,4-triazine ($\mathbf{L^{II}}$) ligands with $AgNO_3$, namely, $[Ag(L^I)_2]NO_3{\cdot}0.5H_2O$ (**1**), $[Ag(L^I)\text{-}PPh_3NO_3]{\cdot}0.5CH_2Cl_2$ (**2**), and $[Ag_2(L^{II})_2(H_2O)_2](NO_3)_2$ (**3**). It was established that **1** can be converted to **2** upon reacting with PPh_3, while no conversion was observed for **3**. The formation of **3** was templated through anion−π-system interactions between the NO_3^- anions and the electron deficient 1,2,4-triazine ring of $\mathbf{L^{II}}$, which play a crucial role in the supramolecular assembly. Furthermore, complex **3** is the first example of a $\mathbf{L^{II}}$-based complex with metal centers.

It is surprising, given a wide potential of both $\mathbf{L^I}$ and $\mathbf{L^{II}}$ for coordination chemistry as well as of their interest as potential building blocks for the fabrication of new materials with interesting and valuable properties, that these ligands remained extremely rare for so long and their chemistry is either poorly studied or completely unexplored. What other surprises are stored in the hidden reserves of coordination chemistry?

ASSOCIATED CONTENT

Supporting Information

The Supporting Information is available free of charge on the ACS Publications website at DOI: 10.1021/acs.cgd.6b00277.

Tables S1−S5 with selected bond and weak interaction lengths and angles, and π−π distances and angles for **1**−**3** (PDF)

Accession Codes

CCDC 1447371−1447373 contains the supplementary crystallographic data for this paper. These data can be obtained free of charge via www.ccdc.cam.ac.uk/data_request/cif, or by emailing data_request@ccdc.cam.ac.uk, or by contacting The Cambridge Crystallographic Data Centre, 12, Union Road, Cambridge CB2 1EZ, UK; fax: +44 1223 336033.

AUTHOR INFORMATION

Corresponding Author

*E-mail: damir.a.safin@gmail.com.

Notes

The authors declare no competing financial interest.

ACKNOWLEDGMENTS

This work was partly supported by the FNRS (Belgium). D. A. Safin and M. G. Babashkina thank WBI (Belgium) for the postdoctoral positions.

REFERENCES

(1) Alkorta, I.; Rozas, I.; Elguero, J. *J. Org. Chem.* **1997**, *62*, 4687−4691.
(2) Gallivan, J. P.; Dougherty, D. A. *Org. Lett.* **1999**, *1*, 103−106.
(3) Schneider, H.-J. *Angew. Chem., Int. Ed. Engl.* **1991**, *30*, 1417−1436.
(4) Gamez, P.; Mooibroek, T. J.; Teat, S. J.; Reedijk, J. *Acc. Chem. Res.* **2007**, *40*, 435−444.
(5) Mooibroek, T. J.; Black, C. A.; Gamez, P.; Reedijk, J. *Cryst. Growth Des.* **2008**, *8*, 1082−1093.
(6) Schottel, B. L.; Chifotides, H. T.; Dunbar, K. R. *Chem. Soc. Rev.* **2008**, *37*, 68−83.
(7) Caltagirone, C.; Gale, P. A. *Chem. Soc. Rev.* **2009**, *38*, 520−563.
(8) Berryman, O. B.; Johnson, D. W. *Chem. Commun.* **2009**, 3143−3153.
(9) Robertazzi, A.; Krull, F.; Knapp, E.-W.; Gamez, P. *CrystEngComm* **2011**, *13*, 3293−3300.
(10) Estarellas, C.; Frontera, A.; Quiñonero, D.; Deyà, P. M. *Angew. Chem., Int. Ed.* **2011**, *50*, 415−418.
(11) Frontera, A.; Gamez, P.; Mascal, M.; Mooibroek, T. J.; Reedijk, J. *Angew. Chem., Int. Ed.* **2011**, *50*, 9564−9583.
(12) Krieger, I. V.; Freundlich, J. S.; Gawandi, V. B.; Roberts, J. B.; Gawandi, V. B.; Sun, Q.; Owen, J. L.; Fraile, M. T.; Huss, S. I.; Lavandera, J.-L.; Ioerger, T. R.; Sacchettini, J. C. *Chem. Biol.* **2012**, *19*, 1556−1567.
(13) Bowman-James, K.; Bianchi, A.; García-España, E. *Anion Coordination Chemistry*; Wiley-VCH, 2012.
(14) Chifotides, H. T.; Dunbar, K. R. *Acc. Chem. Res.* **2013**, *46*, 894−906.
(15) Zhao, Y.; Beuchat, C.; Domoto, Y.; Gajewy, J.; Wilson, A.; Mareda, J.; Sakai, N.; Matile, S. *J. Am. Chem. Soc.* **2014**, *136*, 2101−2111.
(16) Giese, M.; Albrecht, M.; Rissanen, K. *Chem. Commun.* **2016**, *52*, 1778−1795.
(17) Mascal, M.; Armstrong, A.; Bartberger, M. D. *J. Am. Chem. Soc.* **2002**, *124*, 6274−6276.
(18) Alkorta, I.; Rozas, I.; Elguero, J. *J. Am. Chem. Soc.* **2002**, *124*, 8593−8598.
(19) Quiñonero, D.; Garau, C.; Rotger, C.; Frontera, A.; Ballester, P.; Costa, A.; Deyà, P. M. *Angew. Chem., Int. Ed.* **2002**, *41*, 3389−3392.
(20) (a) Demeshko, S.; Dechert, S.; Meyer, F. *J. Am. Chem. Soc.* **2004**, *126*, 4508−4509.
(21) de Hoog, P.; Gamez, P.; Mutikainen, H.; Turpeinen, U.; Reedijk, J. *Angew. Chem., Int. Ed.* **2004**, *43*, 5815−5817.
(22) Kim, D.; Tarakeshwar, P.; Kim, K. S. *J. Phys. Chem. A* **2004**, *108*, 1250−1258.
(23) Kim, D.; Lee, E. C.; Kim, K. S.; Tarakeshwar, P. *J. Phys. Chem. A* **2007**, *111*, 7980−7986.
(24) Kim, D. Y.; Singh, N. J.; Lee, J. W.; Kim, K. S. *J. Chem. Theory Comput.* **2008**, *4*, 1162−1169.
(25) Kim, D. Y.; Singh, N. J.; Kim, K. S. *J. Chem. Theory Comput.* **2008**, *4*, 1401−1407.
(26) Wheeler, S. E.; Houk, K. N. *J. Phys. Chem. A* **2010**, *114*, 8658−8664.
(27) Wheeler, S. E.; Bloom, J. W. G. *J. Phys. Chem. A* **2014**, *118*, 6133−6147.
(28) Quiñonero, D.; Frontera, A.; Deyà, P. M. *ChemPhysChem* **2008**, *9*, 397−399.
(29) Gural'skiy, I. A.; Escudero, D.; Frontera, A.; Solntsev, P. V.; Rusanov, E. B.; Chernega, A. N.; Krautscheid, H.; Domasevitch, K. V. *Dalton Trans.* **2009**, 2856−2864.
(30) Schottel, B. L.; Bacsa, J.; Dunbar, K. R. *Chem. Commun.* **2005**, 46−47.

DOI: 10.1021/acs.cgd.6b00277
Cryst. Growth Des. 2016, 16, 3763−3770

(31) Schottel, B. L.; Chifotides, H. T.; Shatruk, M.; Chouai, A.; Bacsa, J.; Pérez, L. M.; Dunbar, K. R. *J. Am. Chem. Soc.* **2006**, *128*, 5895−5912.
(32) Safin, D. A.; Xu, Y.; Korobkov, I.; Bryce, D. L.; Murugesu, M. *CrystEngComm* **2013**, *15*, 10419−10422.
(33) Safin, D. A.; Tumanov, N. A.; Leitch, A. A.; Brusso, J. L.; Filinchuk, Y.; Murugesu, M. *CrystEngComm* **2015**, *17*, 2190−2195.
(34) Safin, D. A.; Burgess, K. M. N.; Korobkov, I.; Bryce, D. L.; Murugesu, M. *CrystEngComm* **2014**, *16*, 3466−3469.
(35) Safin, D. A.; Holmberg, R. J.; Burgess, K. M. N.; Robeyns, K.; Bryce, D. L.; Murugesu, M. *Eur. J. Inorg. Chem.* **2015**, *2015*, 441−446.
(36) Safin, D. A.; Pialat, A.; Korobkov, I.; Murugesu, M. *Chem. - Eur. J.* **2015**, *21*, 6144−6149.
(37) Safin, D. A.; Pialat, A.; Leitch, A. A.; Tumanov, N. A.; Korobkov, I.; Filinchuk, Y.; Brusso, J. L.; Murugesu, M. *Chem. Commun.* **2015**, *51*, 9547−9550.
(38) Safin, D. A.; Szell, P. M. J.; Keller, A.; Korobkov, I.; Bryce, D. L.; Murugesu, M. *New J. Chem.* **2015**, *39*, 7147−7152.
(39) Safin, D. A.; Frost, J.; Murugesu, M. *Dalton Trans.* **2015**, *44*, 20287−20294.
(40) Kozhevnikov, V. N.; Kozhevnikov, D. N.; Shabunina, O. V.; Rusinov, V. L.; Chupakhin, O. N. *Tetrahedron Lett.* **2005**, *46*, 1791−1793.
(41) Kozhevnikov, D. N.; Shabunina, O. V.; Kopchuk, D. S.; Slepukhin, P. A.; Kozhevnikov, V. N. *Tetrahedron Lett.* **2006**, *47*, 7025−7029.
(42) Safin, D. A.; Mitoraj, M. P.; Robeyns, K.; Filinchuk, Y.; Vande Velde, C. M. L. *Dalton Trans.* **2015**, *44*, 16824−16832.
(43) Tian, A.; Han, Z.; Peng, J.; Dong, B.; Sha, J.; Li, B. *J. Mol. Struct.* **2007**, *832*, 117−123.
(44) Tian, A.-X.; Han, Z.-G.; Peng, J.; Zhai, J.-L.; Dong, B.-X.; Sha, J.-Q. *J. Coord. Chem.* **2007**, *60*, 1645−1654.
(45) Cui, S.; Zuo, M.; Zhang, J.; Zhao, Y.; Tan, R.; Liu, S.; Su, S. *Acta Crystallogr., Sect. E: Struct. Rep. Online* **2011**, *67*, m1706−m1707.
(46) Cui, S.; Zuo, M.; Zhang, J.; Zhao, Y.; Wang, H. *Acta Crystallogr., Sect. E: Struct. Rep. Online* **2012**, *68*, m165.
(47) Spek, A. L. *Acta Crystallogr., Sect. D: Biol. Crystallogr.* **2009**, *D65*, 148−155.
(48) Yang, L.; Powell, D. R.; Houser, R. P. *Dalton Trans.* **2007**, 955−964.
(49) Yao, W.; Eisenstein, O.; Crabtree, R. H. *Inorg. Chim. Acta* **1997**, *254*, 105−111.
(50) Zhang, U.; Lewis, J. C.; Bergman, R. G.; Ellman, J. A.; Oldfield, E. *Organometallics* **2006**, *25*, 3515−3519.
(51) Brookhart, M.; Green, M. L. H.; Parkin, G. *Proc. Natl. Acad. Sci. U. S. A.* **2007**, *104*, 6908−6914.
(52) Huynh, H. V.; Wong, L. R.; Ng, P. S. *Organometallics* **2008**, *27*, 2231−2237.
(53) Saßmannshausen, J. *Dalton Trans.* **2012**, *41*, 1919−1923.
(54) Siddiqui, K. A.; Tiekink, E. R. T. *Chem. Commun.* **2013**, *49*, 8501−8503.
(55) Schöler, S.; Wahl, M. H.; Wurster, N. I. C.; Puls, A.; Hättig, C.; Dyker, G. *Chem. Commun.* **2014**, *50*, 5909−5911.
(56) Holaday, M. G. D.; Tarafdar, G.; Kumar, A.; Reddy, M. L. P.; Srinivasan, A. *Dalton Trans.* **2014**, *43*, 7699−7703.
(57) Scherer, W.; Dunbar, A. C.; Barquera-Lozada, J. E.; Schmitz, D.; Eickerling, G.; Kratzert, D.; Stalke, D.; Lanza, A.; Macchi, P.; Casati, N. P. M.; Ebad-Allah, J.; Kuntscher, C. *Angew. Chem., Int. Ed.* **2015**, *54*, 2505−2509.
(58) Addison, A. W.; Nageswara, R. T.; Reedijk, J.; Van Rijn, J.; Verschoor, G. J. *J. Chem. Soc., Dalton Trans.* **1984**, 1349−1356.
(59) Allen, F. H. *Acta Crystallogr., Sect. B: Struct. Sci.* **2002**, *B58*, 380−388.
(60) CSD version 5.37 (November 2015 + 1 update).
(61) Bondi, A. *J. Phys. Chem.* **1964**, *68*, 441−451.
(62) Rigaku Oxford Diffraction, CrysAlis(Pro) Software system, v 1.171.37.31; Rigaku Corporation, Oxford, UK, 2014.
(63) Sheldrick, G. M. *Acta Crystallogr.* **2015**, *C71*, 3−8.
(64) Bruno, I. J.; Cole, J. C.; Edgington, P. R.; Kessler, M.; Macrae, C. F.; McCabe, P.; Pearson, J.; Taylor, R. *Acta Crystallogr., Sect. B: Struct. Sci.* **2002**, *B58*, 389−397.

DOI: 10.1021/acs.cgd.6b00277
Cryst. Growth Des. 2016, 16, 3763−3770